

Yielding transition of stress controlled granular materials near jamming

Kiwamu Yoshii^{1,2,*}, Takenobu Nakamura³, Michio Otsuki^{4,5},

¹Department of Applied Physics, Tokyo University of Science, 6-3-1, Nijuku, Katsushika-ku, Tokyo 125-8585, Japan

²Department of Physics, Nagoya University, Furo-cho, Chikusa-ku, Nagoya 464-8602, Japan

³National Institute of Advanced Industrial Science and Technology (AIST), 1-1-1 Umezono, Tsukuba, Ibaraki 305-8568, Japan

⁴Graduate School of Engineering Science, Osaka University, 1-3 Machikaneyama, Toyonaka, Osaka 560-8531, Japan

⁵Institute of Science and Engineering, Shimane University, 1060 Nishikawatsu-cho, Matsue, Shimane 690-8504, Japan

Abstract. In this study, we numerically investigate the yielding behavior of frictional granular materials using stress-controlled simulations. The shear stress is applied to the granular materials, which induces shear deformation. When the applied stress is below the yield stress, the shear strain saturates at a finite value; however, it grows indefinitely over time once the stress exceeds the yield stress. Our numerical results suggest that the characteristic strain required for a mechanically stable state diverges discontinuously at the yielding point. The yielding point depends on the interparticle friction coefficient. We further examine how the characteristic strain depends on the distance from the yielding point, revealing a non-monotonic relationship with the interparticle friction coefficient.

1 Introduction

The disordered systems, such as granular materials and colloidal suspensions, exhibit solid-like behavior with rigidity when the packing fraction exceeds a critical value, whereas they behave like fluids below this threshold [1, 2]. This transition, known as the jamming transition, has been extensively studied for many years.

Previous studies have revealed the critical behavior of the shear modulus under infinitesimal shear stress or shear strain near the critical fraction, which characterizes the linear response of the disordered systems [2, 3]. Recently, nonlinear rheological behavior under finite strain, known as softening, has been reported and is attracting increasing attention [4–7].

Jammed materials also exhibit a yielding transition when the applied stress σ_t exceeds the yield stress σ_Y [8]. When $\sigma_t < \sigma_Y$, the shear deformation remains finite, which is known as the arrested state. For $\sigma_t \geq \sigma_Y$, the granular materials yield, and the shear strain grows indefinitely over time, which is called the flow state. Recent studies have investigated the transient dynamics near the yielding transition, focusing on the characteristic strain and time required to reach a mechanically stable configuration in the arrested state [9, 10]. In Ref. [9], a finite-size scaling for the characteristic strain in frictionless granular materials has been proposed, suggesting that the characteristic shear strain follows a power-law behavior as a function of the distance from the yielding point and continuously diverge as $\sigma_t \rightarrow \sigma_Y$. The characteristic time for frictional granular materials has been numerically investigated in Ref. [10], where a non-monotonic dependence

on the interparticle friction coefficient has been reported. However, research on the critical behavior of granular materials near the yielding point remains limited, particularly regarding the characteristic strain in frictional grains.

In this study, we numerically investigate the transient dynamics of jammed frictional granular materials under a constant shear stress. We describe our model and setup in Sec. 2. In Sec. 3, we demonstrate that the characteristic shear strain depends on the shear stress and the interparticle friction coefficient. In Sec. 4, we discuss and summarize our results.

2 Model and Simulation Setup

We perform numerical simulations of a three-dimensional system consisting of frictional granular particles. To prevent crystallization, we consider a 50:50 binary mixture of small and large particles with diameters d_0 and $1.4d_0$. The density of each particle is assumed to be identical, and the mass is proportional to the cube of its diameter. The mass of a particle with diameter d_0 is denoted by m_0 . The time evolution of the position \mathbf{r}_i for the i -th particle is given by

$$m_i \frac{d^2 \mathbf{r}_i}{dt^2} = \sum_{j \neq i} (F_{ij}^n \mathbf{n}_{ij} + F_{ij}^t \mathbf{t}_{ij}). \quad (1)$$

where m_i is the mass of the i -th particle. Here, \mathbf{n}_{ij} and \mathbf{t}_{ij} are the unit normal and tangential vectors at the contact between particles i and j , respectively [11]. The normal and tangential forces are denoted by F_{ij}^n and F_{ij}^t , respectively.

The normal force F_{ij}^n between particles i and j consists of the elastic part F_{ij}^{el} and dissipative part F_{ij}^{diss} as $F_{ij}^n =$

*e-mail: qyoshii@rs.tus.ac.jp

$F_{ij}^{\text{el}} + F_{ij}^{\text{diss}}$. The elastic part is given by

$$F_{ij}^{\text{el}} = k_n(d_{ij} - r_{ij})\Theta(d_{ij} - r_{ij}), \quad (2)$$

while the dissipative part is given by

$$F_{ij}^{\text{diss}} = -\eta_n v_{ij}\Theta(d_{ij} - r_{ij}) \quad (3)$$

with the normal spring constant k_n , the viscous constant η_n , the diameter d_i of the i -th particle, $d_{ij} \equiv (d_i + d_j)/2$, $r_{ij} \equiv r_i - r_j$, and $v_{ij} \equiv (\dot{r}_i - \dot{r}_j) \cdot \mathbf{n}_{ij}$. Here, $\Theta(x)$ is Heaviside's step function satisfying $\Theta(x) = 1$ for $x \geq 0$ and $\Theta(x) = 0$ otherwise.

The tangential force F_{ij}^t is given by

$$F_{ij}^t = \begin{cases} k_t \delta_{ij} - \eta_t v_{ij}^t & (|F_{ij}^t| < \mu_p |F_{ij}^n|), \\ \mu_p F_{ij}^n & (|F_{ij}^t| \geq \mu_p |F_{ij}^n|). \end{cases} \quad (4)$$

Here, the tangential displacement δ_{ij} is given by $\delta_{ij} = \int_{\text{stick}} v_{ij}^t dt$, where the integral is evaluated only if the particles remain in contact. The relative tangential velocity v_{ij}^t is defined as $v_{ij}^t = (\dot{r}_i - \dot{r}_j) \cdot \mathbf{t}_{ij} - \frac{1}{2}(d_i \omega_i + d_j \omega_j)$. Here, k_t is the tangential spring constant, η_t is the tangential viscous constant, ω_i is the angular velocity, and μ_p is the interparticle friction coefficient [11].

We consider a rectangular system with lengths L_x , L_y , and the time-dependent length $L_z(t)$, and impose periodic boundary conditions in the x - and y -directions. Here, L_x and L_y are kept constant, while $L_z(t)$ varies with time t .

The Cauchy stress is given by

$$\sigma_{\alpha\beta}(t) = -\frac{1}{V(t)} \sum_{i < j} r_{ij,\alpha} F_{ij,\beta}, \quad (\alpha, \beta = x, y, z) \quad (6)$$

with $V(t) = L_x L_y L_z(t)$. To control the stress, we adopt the Parrinello-Rahman method with the Lees-Edwards boundary condition in the z -direction [12, 13], using a feedback protocol [14]. The evolution of the shear rate $\dot{\gamma}(t)$ is governed by

$$\frac{d\dot{\gamma}(t)}{dt} = B(S - \sigma_{xz}(t)), \quad (7)$$

where B is the feedback parameter. In this method, $\dot{\gamma}(t)$ evolves so that $\sigma_{xz}(t)$ approaches a constant S . We also control the pressure $P(t) = -\sigma_{zz}(t)$ in the z -direction by adjusting $L_z(t)$ according to

$$\frac{dL_z(t)}{dt} = L_z(t)C(P_t - P(t)), \quad (8)$$

where P_t is the target pressure and C is the feedback parameter.

In the initial state, we choose $L_z(t) = L_{z0}$, and the particles are randomly placed in the rectangular simulation box without any overlap. First, the initial configuration is gradually compressed along the z -direction following Eq. (8) with $\dot{\gamma}(t) = 0$ until a statically compressed state with the target pressure P_t is obtained.

At $t = 0$, we apply a sufficiently small shear stress, $S = \sigma_{t0} = 1.0 \times 10^{-5} k_n d_0^{-1}$, and the system evolves toward mechanical equilibrium according to Eqs. (7) and

(8) during a relaxation time τ , eventually achieving quasi-static shear under constant pressure. For $\tau < t \leq 2\tau$, we set $S = \sigma_t$, where σ_t is the target stress. If σ_t exceeds the yield stress σ_Y , the shear rate $\dot{\gamma}(t)$ remains finite at $t = 2\tau$. In contrast, for $\sigma_t < \sigma_Y$, $\dot{\gamma}(t = 2\tau) \approx 0$. The system is considered to be in the flow state when $\dot{\gamma} > 1.0 \times 10^{-5} \sqrt{k_n/m_0}$, whereas it is classified as the arrested state when $\dot{\gamma} \leq 1.0 \times 10^{-5} \sqrt{k_n/m_0}$.

We use $k_t = (2/7)k_n$, $\eta_n = (2/7)\sqrt{m_0 k_n}$, $\eta_t = (2/7)\eta_n$, $L_x = L_y = 16d_0$, $L_{z0} = 30d_0$, $B = 0.001d_0/m_0$, $C = 0.001d_0(m_0 k_n)^{-1/2}$, and $\tau = 40000\sqrt{m_0/k_n}$. The system consists of $N = 4096$ particles. Note that our system is significantly larger than those used in previous studies [9]. We examine interparticle friction coefficients μ_p in the range of 0.01 to 1.0. The time evolution is numerically simulated using LAMMPS, an open-source molecular dynamics program developed at Sandia National Laboratories, with a time step of $\Delta t = 0.05\sqrt{m_0/k_n}$ [15].

3 Result

Figure 1(a) shows the shear rate $\dot{\gamma}(t)$ as a function of $t - \tau$ for $\mu_p = 0.05$ with $\sigma_t = 2.0 \times 10^{-5} k_n d_0^{-1}$ and $2.2 \times 10^{-5} k_n d_0^{-1}$. For $\sigma_t = 2.2 \times 10^{-5} k_n d_0^{-1}$, $\dot{\gamma}(t) > 0$ for all t , indicating that the system is in the flow state. For smaller σ_t , there is a transient period where $\dot{\gamma}(t) > 0$, but it decays to zero until $t = 2\tau$, indicating that the system is in the arrested state. Figures 1(b) and 1(c) respectively show the shear stress $\sigma_{xz}(t)$ and the pressure $P(t)$ as functions of $t - \tau$ for $\mu_p = 0.05$ with $\sigma_t = 2.0 \times 10^{-5} k_n d_0^{-1}$ and $2.2 \times 10^{-5} k_n d_0^{-1}$. In the flow state ($\sigma_t = 2.2 \times 10^{-5} k_n d_0^{-1}$), the shear stress fluctuates around σ_t for all t , while in the arrested state ($\sigma_t = 2.0 \times 10^{-5} k_n d_0^{-1}$), the fluctuation eventually stops. We note that $P(t)$ remains almost unchanged in both states. This fluctuation in $\sigma_{xz}(t)$ and $P(t)$ may depend on the feedback parameters B and C .

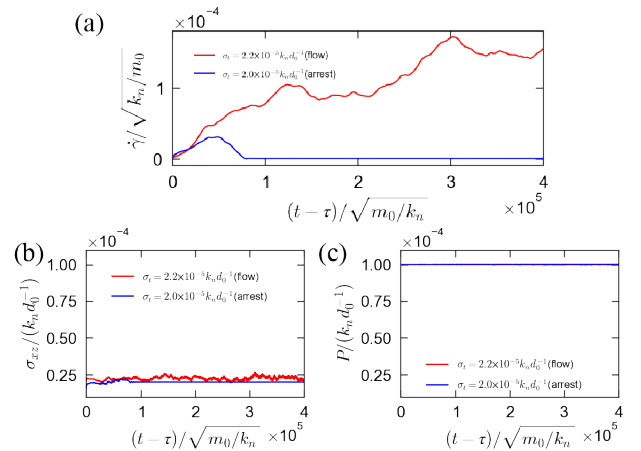


Figure 1. (a) The shear rate $\dot{\gamma}(t)$ as a function of $t - \tau$ for $\mu_p = 0.05$ with $\sigma_t = 2.0 \times 10^{-5} k_n d_0^{-1}$ and $2.2 \times 10^{-5} k_n d_0^{-1}$. (b) The shear stress $\sigma_{xz}(t)$ as a function of $t - \tau$ for $\mu_p = 0.05$ with $\sigma_t = 2.0 \times 10^{-5} k_n d_0^{-1}$ and $2.2 \times 10^{-5} k_n d_0^{-1}$. (c) The pressure $P(t)$ as a function of $t - \tau$ for $\mu_p = 0.05$ with $\sigma_t = 2.0 \times 10^{-5} k_n d_0^{-1}$ and $2.2 \times 10^{-5} k_n d_0^{-1}$.

Figure 1 indicates that the yield stress σ_Y , which distinguishes the flow and arrested states, lies between $\sigma_t = 2.0 \times 10^{-5} k_n d_0^{-1}$ and $2.2 \times 10^{-5} k_n d_0^{-1}$. To characterize the transient dynamics after applying the shear stress near the yielding point, we define the accumulated strain as $\gamma_{MS} = \int_0^{2\tau} \dot{\gamma}(t) dt$. In the arrested state, γ_{MS} remains finite, while it becomes infinite in the flow state for $\tau \rightarrow \infty$. Thus, the inverse γ_{MS}^{-1} is nonzero in the arrested state with $\sigma_t < \sigma_Y$, while $\gamma_{MS}^{-1} \approx 0$ for sufficiently large τ in the flow state with $\sigma_t \geq \sigma_Y$.

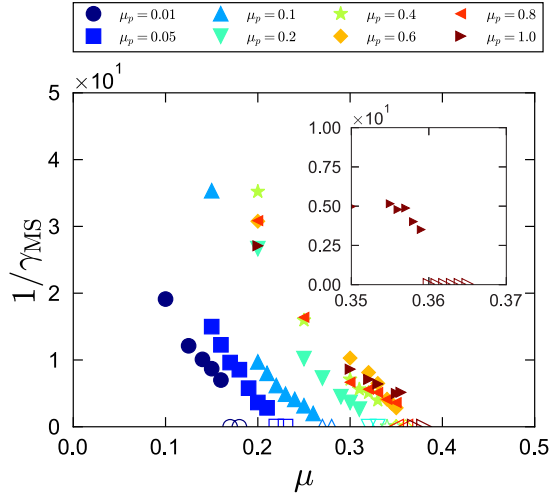


Figure 2. γ_{MS}^{-1} as a function of μ for various values of the interparticle friction coefficient μ_p . Open (closed) symbols correspond to the flow (arrest) state. The inset provides a close-up view near the transition point for $\mu_p = 1.0$.

Following Refs. [9, 10], we use the dimensionless shear stress as a control parameter, defined as

$$\mu = \frac{\sigma_t}{P_t}. \quad (9)$$

Figure 2 shows γ_{MS}^{-1} as a function of μ for various values of the interparticle friction coefficient μ_p . In this figure, closed and open symbols represent the arrested and flow states, respectively. For each μ_p , γ_{MS}^{-1} decreases as μ increases and decays to 0 at the boundary between the arrested and flow states. We define the dimensionless yield stress μ_c as the value of μ at this boundary. At μ_c , γ_{MS}^{-1} discontinuously drops to 0, which indicates that γ_{MS} discontinuously diverges at the yielding point. The inset of Fig. 2 highlights the discontinuous change in γ_{MS}^{-1} near the boundary between the arrested and flowing states. This behavior contrasts with the continuous divergence of γ_{MS} suggested in the finite-size scaling for much smaller frictionless systems in Ref. [9].

Figure 3 shows the dimensionless yield stress μ_c as a function of the interparticle friction coefficient μ_p in simulations under constant shear stress and constant shear rate conditions. In the simulations under constant shear rate, we set $\dot{\gamma} = 1.0 \times 10^{-5} \sqrt{k_n/m_0}$ instead of using Eq. (7), and estimate μ_c as the time-averaged value of $\sigma_{xz}(t)/P(t)$ in the steady state for $\gamma \geq 2$. As μ_p increases, the dimensionless

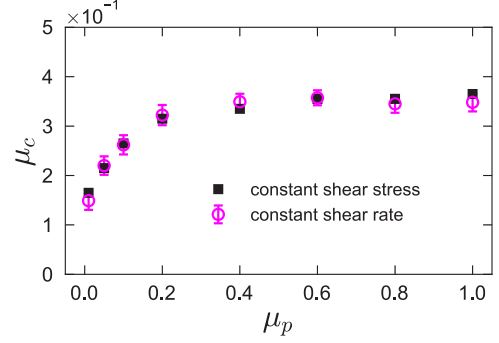


Figure 3. Dimensionless yield stress μ_c as a function of the interparticle friction coefficient μ_p in simulations under constant shear stress and constant shear rate conditions.

yield stress μ_c increases and saturates for $\mu_p > 0.4$ under both conditions.

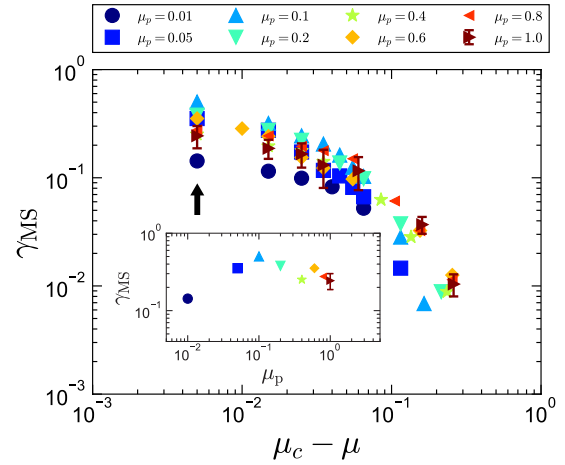


Figure 4. γ_{MS} as a function of $\mu_c - \mu$ for various values of the interparticle friction coefficient μ_p . The inset shows μ_p as a function of γ_{MS} for $\mu_c - \mu = 5.0 \times 10^{-3}$.

Figure 4 shows the characteristic strain γ_{MS} as a function of $\mu_c - \mu$ for various values of the interparticle friction coefficient μ_p . As $\mu_c - \mu$ approaches 0, the slope of the curve decreases, which contradicts the power-law divergence for $\mu \rightarrow \mu_c$ suggested in Ref. [9]. Additionally, we observe a non-monotonic dependence of γ_{MS} on μ_p , as shown in the inset of Fig. 4, which presents γ_{MS} as a function of μ_p for $\mu_c - \mu = 5.0 \times 10^{-3}$. This behavior is similar to the one observed for the characteristic time required to reach the mechanically stable state [10].

4 Discussion and Conclusion

In this study, we numerically investigated the characteristic strain γ_{MS} required for the mechanically stable state in a frictional granular system under a stress-controlled protocol. When the shear stress exceeds the yield stress, the shear rate becomes non-zero, leading to a flow state. In contrast, when the shear stress is below the yield stress, the system remains in the arrested state. We found that γ_{MS}^{-1}

discontinuously decays to 0 as μ increases. This discontinuous change contrasts with the power-law divergence of the shear strain suggested for frictionless grains in Ref. [9]. However, extensive studies of the finite-size effect are needed to clarify the divergence.

The relation between γ_{MS} and $\mu_c - \mu$ exhibits a non-monotonic dependence on the interparticle friction coefficient μ_p . In addition to Ref. [10], a similar non-monotonic dependence has been reported for the relaxation time of granular materials under cyclic shear in Ref. [16]. This non-monotonic dependence has been attributed to the coupling between changes in the contact network and the interparticle friction. This explanation may help to understand the non-monotonic dependence of the shear strain γ_{MS} under a constant shear stress.

We apply shear stress to granular materials in two steps (σ_{t0} and σ_t). However, it is well known that the mechanical properties of disordered systems exhibit protocol-dependent behaviors, such as history-dependent rheological changes [17, 18] and shear jamming induced by initial training [19]. Since the protocols used in this study differ from those used in Refs. [9, 10], the effect of different protocols should be clarified in future work.

The numerical simulations were mainly conducted using the JAXA Supercomputer System Generation 3 (JSS3). A part of the numerical analysis in this work was carried out at the Yukawa Institute Computer Facility. K.Y. is partially supported by JSPS KAKENHI (Grants No.24KJ0110) and The Public Foundation of Chubu Science and Technology Center. M.O. is partially supported by JSPS KAKENHI (Grants No.23K03248).

References

- [1] A.J. Liu, S.R. Nagel, Jamming is not just cool any more, *Nature* **396** (1998). [10.1038/23819](https://doi.org/10.1038/23819)
- [2] M. van Hecke, Jamming of soft particles: geometry, mechanics, scaling and isostaticity, *J. Phys. Condens. Matter* **22**, 033101 (2009). [10.1088/0953-8984/22/3/033101](https://doi.org/10.1088/0953-8984/22/3/033101)
- [3] C.S. O'hern, L.E. Silbert, A.J. Liu, S.R. Nagel, Jamming at zero temperature and zero applied stress: The epitome of disorder, *Phys. Rev. E* **68** (2003). [10.1103/PhysRevE.68.011306](https://doi.org/10.1103/PhysRevE.68.011306)
- [4] M. Otsuki, H. Hayakawa, Avalanche contribution to shear modulus of granular materials, *Phys. Rev. E* **90**, 042202 (2014). [10.1103/PhysRevE.90.042202](https://doi.org/10.1103/PhysRevE.90.042202)
- [5] S. Dagois-Bohy, E. Somfai, B.P. Tighe, M. Van Hecke, Softening and yielding of soft glassy materials, *Soft Matter* **13**, 9036 (2017). [10.1039/C7SM01846K](https://doi.org/10.1039/C7SM01846K)
- [6] M. Otsuki, H. Hayakawa, Softening and residual loss modulus of jammed grains under oscillatory shear in an absorbing state, *Phys. Rev. Lett.* **128**, 208002 (2022). [10.1103/PhysRevLett.128.208002](https://doi.org/10.1103/PhysRevLett.128.208002)
- [7] T. Kawasaki, K. Miyazaki, Unified understanding of nonlinear rheology near the jamming transition point, *Phys. Rev. Lett.* **132**, 268201 (2024). [10.1103/PhysRevLett.132.268201](https://doi.org/10.1103/PhysRevLett.132.268201)
- [8] D. Bonn, M.M. Denn, L. Berthier, T. Divoux, S. Manneville, Yield stress materials in soft condensed matter, *Rev. Mod. Phys.* **89**, 035005 (2017). [10.1103/RevModPhys.89.035005](https://doi.org/10.1103/RevModPhys.89.035005)
- [9] A.H. Clark, J.D. Thompson, M.D. Shattuck, N.T. Ouellette, C.S. O'Hern, Critical scaling near the yielding transition in granular media, *Phys. Rev. E* **97**, 062901 (2018). [10.1103/PhysRevE.97.062901](https://doi.org/10.1103/PhysRevE.97.062901)
- [10] I. Srivastava, L.E. Silbert, G.S. Grest, J.B. Lechman, Flow-arrest transitions in frictional granular matter, *Phys. Rev. Lett.* **122**, 048003 (2019). [10.1103/PhysRevLett.122.048003](https://doi.org/10.1103/PhysRevLett.122.048003)
- [11] S. Luding, Cohesive, frictional powders: contact models for tension, *Granul. Matter* **10**, 235 (2008). [10.1007/s10035-008-0099-x](https://doi.org/10.1007/s10035-008-0099-x)
- [12] M. Parrinello, A. Rahman, Polymorphic transitions in single crystals: A new molecular dynamics method, *J. Appl. Phys.* **52**, 7182 (1981). [10.1063/1.328693](https://doi.org/10.1063/1.328693)
- [13] D. Evans, G. Morriss, Non-equilibrium statistical mechanics of liquids (2008)
- [14] R. Cabriolu, J. Horbach, P. Chaudhuri, K. Martens, Precursors of fluidisation in the creep response of a soft glass, *Soft Matter* **15**, 415 (2019). [10.1039/C8SM01432A](https://doi.org/10.1039/C8SM01432A)
- [15] S. Plimpton, Fast parallel algorithms for short-range molecular dynamics, *J. Comput. Phys.* **117**, 1 (1995). [10.1006/jcph.1995.1039](https://doi.org/10.1006/jcph.1995.1039)
- [16] Q. Mao, Y. Wang, W. Kob, Dynamic constraints predict the relaxation of granular materials, arXiv preprint arXiv:2405.09078 (2024). [10.48550/arXiv.2405.09078](https://doi.org/10.48550/arXiv.2405.09078)
- [17] M. Otsuki, H. Hayakawa, Critical scaling near jamming transition for frictional granular particles, *Phys. Rev. E* **83**, 051301 (2011). [10.1103/PhysRevE.83.051301](https://doi.org/10.1103/PhysRevE.83.051301)
- [18] M. Grob, A. Zippelius, C. Heussinger, Rheological chaos of frictional grains, *Phys. Rev. E* **93**, 030901 (2016). [10.1103/PhysRevE.93.030901](https://doi.org/10.1103/PhysRevE.93.030901)
- [19] M. Otsuki, H. Hayakawa, Shear jamming, discontinuous shear thickening, and fragile states in dry granular materials under oscillatory shear, *Phys. Rev. E* **101**, 032905 (2020). [10.1103/PhysRevE.101.032905](https://doi.org/10.1103/PhysRevE.101.032905)